GT2019-90484

A THIRD-GENERATION SWIRL-VENTURI LEAN DIRECT INJECTION COMBUSTOR WITH A PREFILMING PILOT INJECTOR

K.M. Tacina and D.P. Podboy
Engine Combustion Branch
NASA Glenn Research Center
Cleveland, Ohio 44135
Email: kathleen.m.tacina@nasa.gov

F.P. Lee and B. Dam
Woodward, FST
Zeeland, MI 49464

ABSTRACT

This paper presents experimental results for a low-NO_x aero gas turbine combustor, in particular, a third-generation swirl-venturi lean direct injection (SV-LDI-3) combustor concept called V4. The purpose of testing was three-fold. First, to evaluate the combustor against the 80% NO_x reduction goal set by NASA's AATT project. Second, to compare V4 to a previous SV-LDI-3 combustor concept called V3, especially at low power conditions. Third, to examine the accuracy of a type of correlation equation frequently used by engine systems analysis groups to estimate NO_x emissions. All three testing goals were met. For the first testing goal, with an estimated NO_x reduction of 85%-90%, SV-LDI-3 V4 surpassed the AATT goal. For the second goal, however, V4 did not perform better than V3 at low power conditions. For the third goal, it was found that a major assumption of the correlation equations — a simple dependence on combustor inlet pressure — did not hold.

INTRODUCTION

Aircraft emissions of the oxides of nitrogen (NO_x) have a harmful effect on human health and the environment. At ground level, NO_x emissions contribute to smog and ozone formation. In the troposphere, NO_x emissions are the third most important greenhouse gas. Furthermore, the radiative impact per unit of NO_x emissions is much higher at altitude than at ground level [1]. In the stratosphere, NO_x emissions destroy the protective ozone layer.

Due to harmful effects of NO_x emissions, NASA's Advanced Air Transport Technology (AATT) project had NO_x reduction as one of its major goals. In particular, AATT sought to develop a small-core combustor for a nominal 133 kN engine that would reduce NO_x emissions by 80% with respect to the CAEP/6 standard. NASA's AATT project has pursued two combustor concepts to meets its NO_x reduction goals. The first concept is axially controlled stoichiometry (ACS) [2,3]. The second concept is the one studied in this paper: lean direct injection (LDI). As defined for aero gas turbine engines, LDI is a fuel-lean combustion concept in which the fuel is injected directly into the combustion zone with no geometrically-separated premixing zone [4, 5]. In LDI, all of the combustion air enters the combustor through the dome. As in other fuel-lean combustors, LDI requires rapid and uniform fuel-air mixing to minimize local near-stoichiometric regions that produce high NO_x emissions. Since it does not have a separate premixing zone, LDI promotes this rapid fuel-air mixing by replacing one traditionally-sized fuel-air mixer with several smaller fuel-air mixers. This is called multi-point LDI [6–15].

This paper focuses on one particular multi-point LDI concept, called SV-LDI-3 V4, V4 for short. Testing of SV-LDI-3 V4 had three main goals. First, compare NO_x emissions results to the CAEP/6 standard to see if it met the AATT 80% NO_x reduction goals. Second, compare SV-LDI-3 V4 to another SV-LDI-3 concept called V3. Third, evaluate the accuracy of an empirical equation used to estimate NO_x emissions at high power conditions.

This correlation equation gives the NO_x emissions index (NO_x, EI) as a function of the combustor inlet pressure p_3, combustor inlet temperature T_3, air pressure drop across the combustor dome $\Delta p/p_3$, and adiabatic flame temperature T_{ad}. In particular, the correlation equation is of the form $NO_x, EI = p_3^n exp(T_3/a)h(\Delta p/p_3, T_{ad})$.

From a combustion science perspective, this type of correlation equation is lacking because the form of the equation does not capture the physics. For example, changing the combustor pressure while keeping the equivalence ratio and other combustor parameters constant, has a complex effect on the combustion process. The droplet size, turbulent length and time scales, and reaction rates all change. Thus, the effect of, say, doubling the inlet pressure may vary depending on other combustor conditions, such as equivalence ratio. A similar argument can be made for other combustor inlet conditions such as combustor inlet temperature.

Nevertheless, equations of the form NO_x, EI = $f(p)g(T)h$(other parameters) are widely used by climate scientists and engine systems analysts to estimate aircraft engine NO_x emissions [16, 17]. The effect of p_3 and T_3 are sometimes used directly; examples include the empirical equations reported in this paper as well as the T_3-p_3 method. Other times, the effects of p_3 and T_3 are approximated using ambient conditions at cruise and the aircraft Mach number, as in the Boeing fuel flow method 2 and the DLR fuel flow method [17]. Furthermore, NO_x correlation equations can be continue to be used for many years. For example, in 1997 Lukachko and Waitz estimated the effect of engine aging on NO_x emissions using correlation equations published almost 20 years before, in the late 1970s [18].

In addition, much of the data from tests of realistic gas turbine combustor concepts is proprietary, especially data taken at elevated pressure and temperature. Even if the emissions data is published, the data is often presented as a function of the engine power setting (e.g., 100% power) because the combustor inlet conditions are often proprietary. Since the both the emissions results and combustor inlet conditions are open for this test, they may help give engine systems analysts and climate scientists a better sense of the uncertainty involved in using simple equations to estimate the effect of pressure and temperature on NO_x emissions.

EXPERIMENTAL HARDWARE AND FACILITIES

This section describes the experimental hardware and facility and lists the combustor conditions for the NASA N+3 engine cycle. Since the facility and engine cycle are the same ones used for previous testing and the hardware is similar, parts of this section are nearly identical to the one in Reference [14].

Combustor configuration: SV-LDI-3

This paper focuses on one LDI concept, called SV-LDI-3 V4. SV-LDI-3 V4 belongs to a family of LDI designs called swirl-venturi LDI [8, 12–15]. Swirl-venturi (SV) LDI designs are distinguished from other LDI concepts by having a converging-diverging venturi downstream of each air swirler. The evolution of the SV-LDI family of combustor concepts is described below and shown in Fig. 1. SV-LDI designs successfully reduced NO_x emissions at high power conditions. However, the original SV-LDI designs (SV-LDI-1) had two major disadvantages: poor low power operability and a complex, multi-branch fuel stem [8]. The second generation of SV-LDI designs (SV-LDI-2) improved the low power operability by better isolating the pilot fuel-air mixer [12, 13]. However, SV-LDI-2 still had a complex, multi-branched fuel stem that would make the thermal management of the fuel difficult. The third generation of SV-LDI, SV-LDI-3, replaces the complex, multi-branched fuel stem with a single, multi-injection-point fuel stem. This both simplifies fuel stem design and improves the thermal management of the fuel.

A single "cup" of a SV-LDI-3 combustor consists of a pilot fuel-air mixer surrounded by multiple main fuel-air mixers. In particular, the pilot is surrounded either by 6 main fuel-air mixers (a "7-point" cup, see Fig. 1d-e) or 4 main fuel-air mixers (a "5-point" cup). Since third-generation SV-LDI targets a small-core engine, the fuel-air mixers must be tightly packed. To accomplish the tight packing, 7-point and 5-point cups alternate.

Since each cup is not identical, the flametube tests were done with multiple cups instead of a single cup. Therefore, a 3-cup sector was tested in the CE-5 medium pressure flametube. The 3-cup sector is composed of two 7-point cups and one 5-point cup, as shown in Fig. 2.

Each cup is fed by a single, multi-injection-point fuel stem. Each of these fuel stem contains three fuel lines that can be controlled separately. For the 5-point cup, one fuel line feeds the pilot, the second feeds the two top mains, and the third feeds the two bottom mains. For the 7-point cup, one fuel line feeds the pilot, the second feeds the three inner mains, and the third feeds the three outer mains.

The fuel-air mixers are grouped into four stages. The first stage is made up of all the pilots. The second stage, called main 1, is made up of the four mains in the 5-point cup. The third stage is comprised of the three inner mains in each of the 7-point cups. The fourth stage is comprised of the three outer mains in each of the 7-point cups. The stages are labeled in Fig. 2.

V4 The description of SV-LDI-3 above applies to both the V3 configuration reported previously [14] and the V4 configuration reported here. V4 differs from V3 in three ways. First, a small slit was purposely added to one of the pilot cups. This slit was designed to eliminate cracking of the pilot cups observed
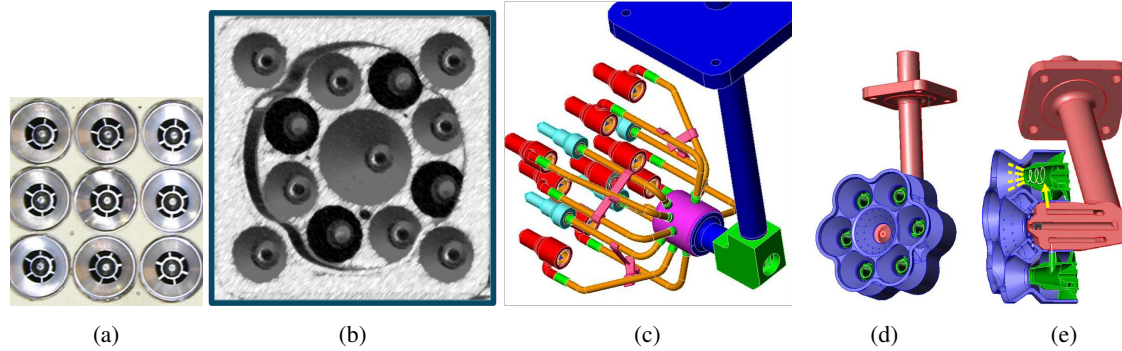
FIGURE 1: Evolution of swirl-venturi (SV-) LDI. Shown are:(a) the dome face of first-generation SV-LDI, with all fuel-air mixers identical except for swirler-vane angle and orientation; (b) the dome face of a second-generation SV-LDI configuration, featuring a larger, recessed pilot fuel-air mixer for improved low-power operability; (c) the multi-branched fuel stem used in second-generation SV-LDI configurations; (d) the dome face of a third-generation SV-LDI configuration; and (e) a cut-out side view of a third-generation SV-LDI configuration showing the single, multi-injection-point fuel stem.
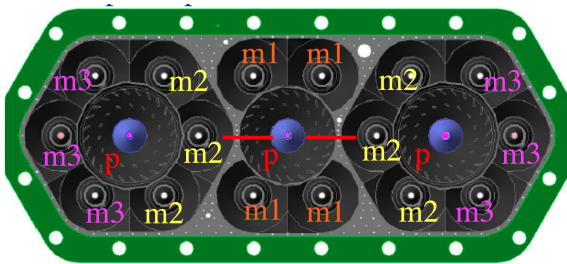
FIGURE 2: The 19-point V4 SV-LDI configuration. The labels indicate the stage of each fuel-air mixer: p=pilot, m1=main 1, m2=main 2, and m3=main3. The location of the slit is indicated by the red lines.

in the earlier version. Second, the pilot fuel injectors have been changed from pressure atomizers (simplex) used in V3 to a pre-filming design. The pilot design was changed because CFD simulations of V3 showed a high percentage of the total NO_x emissions came from the pilot cups [19–21]. Third, the flow number of each fuel injector was increased.

For V4, overall effective area, AC_d, is 1685 mm^2. The AC_ds for the pilot stage, the main 1 stage, the main 2 stage, and the main 3 stage are 248 mm^2, 359 mm^2, 539 mm^2, and 539 mm^2, respectively. The mass flow of air going to each stage is determined by the aerodynamics. In other words, there is no way of independently controlling the air flow to each stage. The percentage of the total air flow going to each stage is taken to be constant at all combustor conditions and is determined using the ratio of AC_d for that stage to the overall AC_d.

For V4, both the airpath and the fuel tips were built using additive manufacturing.

CE-5 Stand 1 intermediate pressure flametube These tests were done on Stand 1 of the CE-5 intermediate pressure combustion facility flametube at NASA Glenn Research Center. The flametube has a cast ceramic liner. This facility can supply nonvitiated air preheated to 922 K at pressures up to 19.0 bar[1].

Stand 1 of CE-5 could support up to three fuel circuits when this test was done. The first fuel circuit fed the pilot stage. The second fuel circuit fed main 1, which are the 4 main fuel-air mixers in the center 5-point cup. Except at the 30% ICAO power condition, the third fuel circuit fed both of the 7-point main stages, main 2 and main 3. At the 30% power condition, the third fuel circuit fed only the inner 7-point main stage, main 2; the outer 7-point fuel stage, main 3, was unfueled. Refer to Fig. 2.

Although the CE-5 facility has the ability to use both Jet-A and alternative liquid fuels, only Jet-A was used in this test.

Testing Strategy Test conditions were based on the NASA N+3 cycle combustor inlet conditions, given in Table 1; test conditions are shown in Fig. 3. Since the CE-5 Stand 1 flametube could not reach the inlet pressure required for the 85% and 100% ICAO power conditions, testing was done at the correct inlet temperature but a lower inlet pressure.

Looking at Fig. 3 leads to the question: Why was testing done at only one pressure for the 100% power inlet temperature? The answer is that testing at three pressures was planned, but testing ended prematurely due to a small crack in the cast ceramic liner. Although testing ended prematurely, the data collected was sufficient to accomplish all three goals for this test. No further testing of V4 is planned. Since V4 was not better than

---

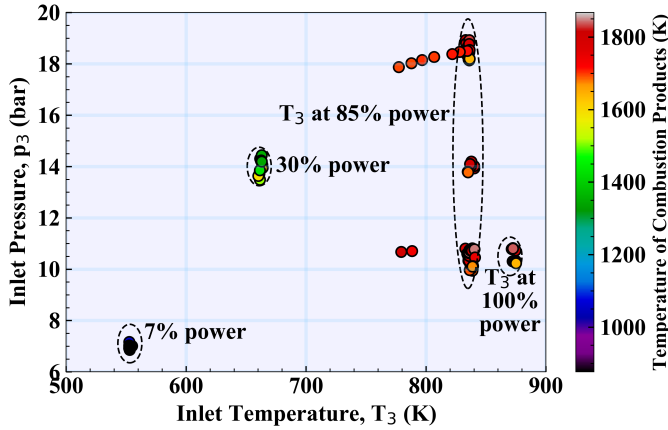[1] 1 bar = 10^5 Pa = 100 kPa = 0.1 MPa

FIGURE 3: Test conditions for the SV-LDI-3 V4 configuration.

V3 at low power conditions, any further SV-LDI-3 testing would incorporate further design changes ("V5").

The combustor air pressure drop was kept near 4% at all conditions.

TABLE 1: NASA N+3 small-core cycle for an engine with 30,000 lbf (133 kN) rated thrust, giving the combustor inlet pressure p$_3$, combustor inlet temperature T$_3$, and combustor equivalence ratio ϕ_{eng}. To calculate the flametube equivalence ratio ϕ_{ft} and flametube combusted gas temperature T$_{\text{ft}}$, twenty percent combustor liner cooling is assumed. In other words, $\phi_{\text{ft}} = \frac{1}{0.8}\phi_{\text{eng}} = 1.25\phi_{\text{eng}}$.

Condition	p$_3$ (bar)	T$_3$ (K)	ϕ_{eng}	ϕ_{ft}	T$_{\text{ft}}$ (K)
7% ICAO	7.1	553	0.103	0.128	890
30% ICAO	14.1	661	0.186	0.233	1,231
85% ICAO	32.8	835	0.325	0.402	1,727
100% ICAO	38.1	870	0.354	0.442	1,832
Cruise	18.3	827	0.392	0.490	1,887
Top of Climb	19.4	834	0.377	0.471	1,858
Rolling Takeoff	44.3	957	0.446	0.558	2,107

DATA ACQUISITION AND ANALYSIS
Steady-State Data Acquisition

Steady-state data was acquired at a rate of 1 Hz using the NASA Glenn ESCORT real-time data acquisition system. It recorded facility conditions such as temperature and pressure as well as gaseous emissions.

Gaseous emissions were collected using a 5-hole probe connected to a gas bench. The probe was located 19.7-cm downstream of the combustor dome, and the 5 holes were spaced 2-cm apart. All 5 holes were on the centerline of the long axis of the combustor, and the center hole was directly downstream of the center of the middle pilot.

The gas bench followed the SAE ARP-1255D [22] standard as closely as possible. The measured combustion products are CO_2, CO, O_2, NO, NO_2, NO_x, and, at low power conditions, UHC. The NO, NO_2, and NO_x measurements were made in duplicate, with two nominally-identical analyzers.

Data Processing

Post-processing followed the SAE ARP-1533B [23] standard. Adiabatic flame temperatures are calculated using the Chemical Equilibrium for Applications (CEA) equilibrium code [24, 25].

Fuel-air ratio: metered vs. gas analysis Fuel-air ratios, equivalence ratio, and flame temperatures can be calculated based either on the gaseous emissions or on the metered fuel and air flowrates. *Unless otherwise specified, these values are based on the gaseous emissions.* Using the gaseous emissions for these calculations should partially compensate for any uneven fuel sampling. If the fuel-air ratio from gaseous emissions is higher than the metered value, the gas sample had a higher fuel-air ratio than the average for the flametube. Such a sample would be expected to also have higher NO_x concentration than the average across the flametube. Similarly, a sample with a lower than metered fuel-air ratio would be expected to have a lower NO_x concentration.

Except at 7% and 30% ICAO power conditions, the fuel-air ratios from metering and from gaseous emissions are typically within 5% of each other. Due to the relative locations of the holes in the emissions probe and the main stages, the two calculations of fuel-air ratios were expected to be more than 5% off at the 30% ICAO power conditions. However, these two calculations were expected to be close at the 7% condition. Despite this discrepancy, even at 7% and 30% power conditions, the data quality is sufficient for estimating the LTO NO_x emissions and for comparing the performance of the V4 and V3 configurations[2].

---

[2]but care should be taken when comparing this low power data to CFD simulations

Unburned hydrocarbons At high power points when unburned hydrocarbon (UHC) measurements were not available[3], UHC emissions were estimated in order to estimate combustion efficiency. For high power conditions, LDI designs typically have very low UHC emissions. Therefore, combustion efficiency is calculated by assuming the UHC emissions index is 20% of the CO emissions index. Based on previous experience, this probably overestimates UHC emissions.

LTO NO$_x$ calculations

NASA's AATT project has the goal of reducing NO$_x$ emissions by 80% with respect to the CAEP/6 standard. The CAEP standards are used by the International Civil Aviation Organization (ICAO) to set the maximum allowable For engines with a pressure ratio between 30 and 82.6 and a maximum rated thrust greater than 89 kN, the CAEP/6 standard uses the following equation to set the maximum NO$_x$ emissions over the landing-takeoff (LTO) cycle:

$$D_p/F_{00} = -1.04 + 2.0\pi_{00}, \tag{1}$$

where D_p/F_{00} is the NO$_x$ severity parameter, D_p is the maximum LTO NO$_x$ emissions in grams, F_{00} is the maximum rated thrust in kN, and π_{00} is the pressure ratio at take-off at sea level static conditions. The NASA AATT N+3 engine cycle has an operating pressure ratio of 55 and a rated thrust of 30,000 lbf (133 kN), so the maximum allowable NO$_x$ severity parameter D_p/F_{00} is 108.96. Therefore, to meet the AATT project goal, the NO$_x$ severity parameter for needs to be below 21.8.

The experimental NO$_x$ severity parameter is calculated using the formula:

$$D_p/F_{00} = \frac{1}{F_{00}} \sum_i t_i w_{f,i} \text{EINOx}_i,, \tag{2}$$

where i refers to the ICAO power setting, t_i is the time at that power setting as defined in the CAEP/6 standard and given in Table 3, $w_{f,i}$ is the fuel flow, and EINOx_i the NO$_x$ emissions index.

RESULTS AND DISCUSSION

One important qualitative observation can be made about the SV-LDI-3 V4 hardware: the small slit added to the center pilot cup did indeed prevent the pilots from cracking.

A second important observation is that combustion dynamics were typically small. For the maximum component of the

---

[3]due to the data acquisition system not communicating properly with the UHC analyzer

power spectrum, the peak-to-peak value is typically less than 0.07 bar (less than 1% of the inlet pressure).

The rest of the results are organized by the ICAO power conditions because these conditions represent different regimes of combustor operation.

Idle: 7% power

The ICAO 7% power condition is close to an idle condition. Figure 4 shows gaseous emissions at the 7% power inlet temperature and pressure. At 7% power, the equivalence ratio is 0.128. This is well below the equivalence ratio needed to maintain a stable flame with Jet-A fuel in an aero gas turbine combustor. Therefore, only the pilot fuel-air mixers are fueled. This would lead to a local equivalence ratio of 0.87 at the pilots if no mixing occurred between the air going through the pilot and main fuel-air mixers. If there is mixing, the levels of CO and UHC would be expected to rise due to quenching of the flame. NO$_x$ levels would go down due to a lower local equivalence ratio. If the mixing is high enough, the flame might even become unstable.

As Fig. 4 shows, V4 had low NO$_x$ emissions but high CO and UHC emissions. At the 7% power overall equivalence ratio of 0.128, the NO$_x$ emissions were only 3.45 g/kg but the CO and UHC emissions were 153 and 23 g/kg, respectively. This led to a calculated combustion efficiency of 94%, unacceptably low. Despite this low combustion efficiency, the flame appeared to be stable.

Comparison of idle performance with previous designs Low power conditions have generally been problematic for LDI configurations. Due to the rapid and uniform fuel-air mixed required to achieve low NO$_x$ emissions at high power, the flame can be quenched at low power. The first-generation SV-LDI-1 configurations could not maintain a stable flame at idle conditions. Second- and third generation SV-LDI-2 and -3 configurations added pilot fuel-air mixers with extended venturis that partially isolated pilot fuel-air mixers from the main fuel-air mixers. With this pilot isolation, all SV-LDI-2 and -3 configurations were able to maintain a stable flame at idle conditions. Although the combustion efficiency was lower than desired (97-98% vs 99+%), it was acceptable for all SV-LDI-2 configurations and for the SV-LDI-3 V3 configuration.

However, the V4 configuration had only 94% combustion efficiency, which was not only unacceptable but also lower than expected. The expectation was that, by changing from the simplex fuel injectors used for the V3 pilot to the prefilming pilot fuel injectors used in V4, the *local* fuel-air mixing in the pilot would improve but the mixing between the pilot and main fuel-air mixers would remain about the same. This would decrease NO$_x$ emissions without decreasing combustion efficiency. Instead, the decrease in NO$_x$ emissions was accompanied by a large increase in CO and UHC emissions. As shown in Fig. 4, even
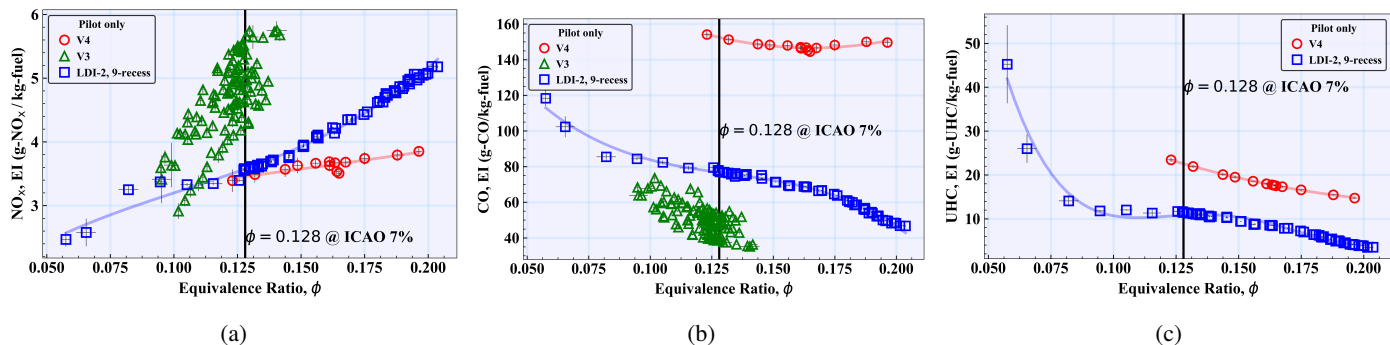
FIGURE 4: Gaseous emissions at the 7% power ICAO point: (a) NO_x, (b) CO, and (c) UHC. V4 is compared to V3 and to a second-generation SV-LDI configuration. The black vertical line indicates the equivalence ratio at the 7% ICAO power condition, $\phi = 0.123$.

when V4 is compared with V3 at the same level of NO_x emissions instead of at the same equivalence ratio, the CO emissions from V4 are nearly double those from V3. Reducing the NO_x emissions does not necessary increase the CO and UHC emissions, as shown by comparing the V4 emissions to the emissions from the SV-LDI-2 9-recess configuration. Although the V4 NO_x emissions are similar the those of this SV-LDI-2 configuration at the 7% power conditions, the V4 CO and UHC emissions are about double those of SV-LDI-2.

Since only emissions were measured, we can only hypothesize about the physical explanation for the increased CO and UHC emissions/decreased combustion efficiency. One possible explanation is that the V4 flame front is further downstream and the combustion air going through the pilot fuel-air mixers has mixed with the air going through the main fuel-air mixers. This would lower the local equivalence ratio, causing the NO_x emissions to decrease and the CO and UHC emissions to increase. A change in flame location could be caused by changing from a simplex to a prefilming fuel injector; this change would change the the initial fuel droplet size and the droplet breakup. In addition, the small slit in the center pilot could be causing additional quenching. Optical diagnostics will be used to better understand the pilot fuel-air mixing and will influence future designs.

Approach: 30% power

Figure 5 shows gaseous emissions at the 30% power temperature and pressure. The 30% power condition corresponds to approach. For this 30% power condition only, the discussion of the emissions results changes significantly depending on whether the equivalence ratio is calculated based on the metered fuel and air flow rates or the gaseous emissions. Therefore, emissions results are plotted against the equivalence ratio calculated by fuel and air metering (bottom row) as well as by gaseous emissions (top row).

At the 30% power condition, the overall equivalence ratio is 0.233, as indicated by the vertical black line. Just as was the

case for the 7% power condition, the equivalence ratio is too low to have a stable flame, so only some of the fuel-air mixers are fueled. To minimize NO_x emissions, the testing strategy was to fuel as many stages as possible while simultaneously keeping the CO and UHC emissions low. For 30% power, two fueling schemes were tested: pilot, main 1, and main 2 fueled; and only pilot and main 2 fueled.

For each fueling scheme, the minimum equivalence ratio was defined as the equivalence ratio where the CO spiked. The minimum equivalence ratio is determined from the fuel-air metering instead of the gaseous emissions because it should not depend on how representatively the emissions are sampled; unrepresentative sampling can have a large effect of the magnitude of the CO spike but should have a much smaller effect on the equivalence ratio at which the spike occurs. For both fueling strategies tested, the CO spike occurred at a higher equivalence than the target equivalence equivalence ratio of 0.233.

NO_x emissions can be estimated using either the equivalence ratio from gas analysis, ϕ_{ga} or the one from metering, ϕ_{met}. At the 30% equivalence ratio of 0.233, the NO_x based on ϕ_{met} is 5 g/kg. The NO_x based on ϕ_{ga} can be found by extrapolation and is 2.62 g/kg for the pilot-main 1-main 2 fueling scheme and 2.88 g/kg for the pilot-main 2 only fueling scheme. The combustion efficiency based on ϕ_{met} is 96%, which is unacceptably low. Due to the spikes in CO and UHC, the combustion efficiency based on ϕ_{ga} cannot be reliably estimated.

A third fueling scheme was planned but not tested due to the premature end to testing. In this third fueling scheme, only pilot and main 1 are fueled.[4] If this fueling scheme had been tried, it is likely to have easily reached the target equivalence ratio of 0.233. This equivalence ratio is only 7% lower than the CO spike (at ϕ_{ga}=0.25) for the pilot-main 2 fueling scheme. How-

---

[4]Based on experience with V3, this third fueling scheme — only pilot and main 1 fueled — was expected to be the most stable and have the highest combustion efficiency. However, since the other two fueling schemes had the potential to produce lower NO_x emissions, they were tried first.
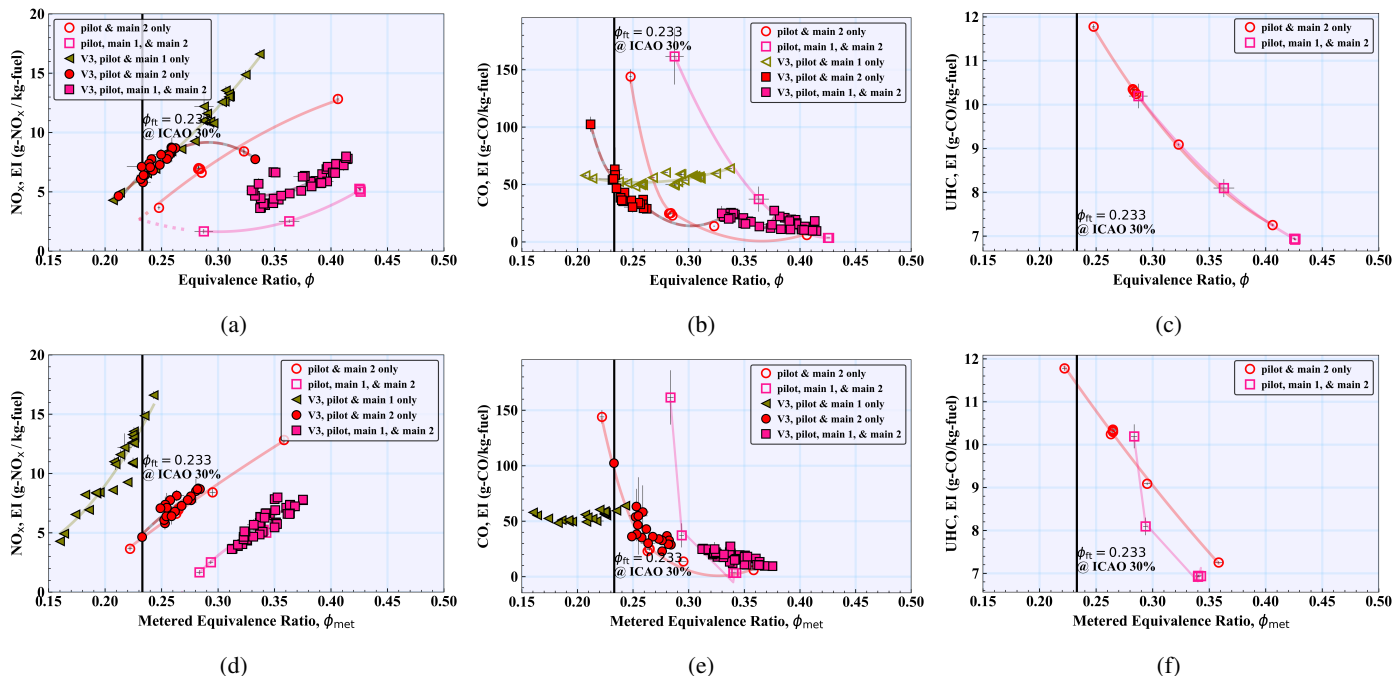
FIGURE 5: Gaseous emissions at the 30% power ICAO point. Emissions are given as a function of the equivalence ratio as calculated from gas analysis (top row) and the equivalence ratio calculated using the metered values of fuel and air (bottom row).

ever, since the main 1 stage has 4 fuel-air mixers whereas the main 2 stage has 6 fuel-air mixers, the local equivalence ratio for the pilot-main 1 fueling scheme is much higher[5]. If we had tried the pilot-main 1 only fuel staging, we estimate the NO_x emissions would have been between 2.8 and 3.0 g/kg based on extrapolations of the other two fueling schemes. For calculating the LTO NO_x emissions, we will assume 3 g/kg. Estimating combustion efficiency for this third fueling scheme is harder. Due to the higher local equivalence ratio, it probably would have been considerably higher. Two very rough estimates of combustion efficiency can be made. First, using the values of CO and UHC for the pilot-main 2 fueling scheme at ϕ_{ga}=1.3×0.233=0.3, the combustion efficiency is estimated to be 98.6%. Second, using the CO value from V3 and the same UHC value, the combustion efficiency is estimated to be 97.7%.

Overall, the V4 emissions are similar to those of V3. The 30% power point was difficult for both V4 and V3. This 30% point approximates approach conditions, and it is important for aero engine combustors to operate well at all points on the flight envelope. Therefore, it might be necessary to change the design of SV-LDI-3 configurations to accommodate this point. On the other hand, although the 30% ICAO power point corresponds to approach, it is not approach. The ICAO power conditions can

sometimes be significantly different than actual points on the engine cycle[6]. Before changing the design, the engine cycle should be analyzed in more detail.

High power: ICAO 85% and 100% power points

At high power conditions, all fuel-air mixers are fueled. As stated in the section describing CE-5 Stand 1 above, three fuel circuits were available. The hardware was plumbed so that the fuel going to the pilot stage fuel-air mixers, to the main 1 stage fuel-air mixers, and to the main 2 and 3 stage fuel-air mixers could be controlled independently. This allowed the fuel to be shifted from one stage to another to minimize NO_x emissions. Based on previous experience, the minimum NO_x emissions were expected when all fuel-air mixers had the nearly same equivalence ratio. Despite this, the local equivalence ratio was varied for two reasons. First, to confirm that NO_x is indeed minimized when all fuel-air mixers have approximately the same equivalence ratio. Second, to improve the quality of the NO_x correlation equations. Previous experience has shown that separating the terms for the pilot and main stages greatly improves the quality of the correlations [12–14]. Varying the equivalence ratio of the pilots relative to the mains allows us to separate the effect of the pilots and the mains on NO_x emissions.

---

[5]about 30% higher if the fuel flow rates are set so that the local equivalence ratio is the same for all fuel-air mixers

[6]For example, parasitic losses are not included. Conversation with Scott Jones of the Propulsion System Analysis Branch at NASA Glenn Research Center.
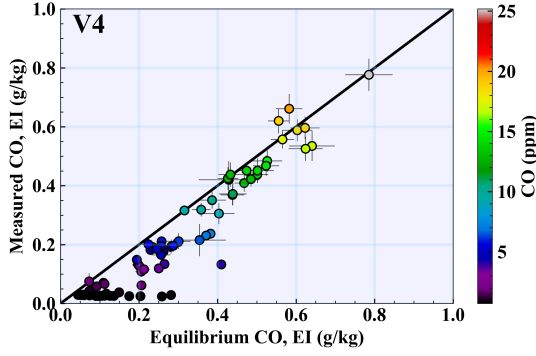
FIGURE 6: CO emissions at high power, compared to equilibrium values.

This subsection is organized as follows. First, the CO emissions are analyzed. Next, the effect of fuel staging is examined. Fuel staging is defined as varying the local equivalence ratio of one fuel-air mixer stage relative to another. Here, the local equivalence ratio of the pilot stage is varied relative to the main stages; all main stages are kept at the same local equivalence ratio. After that, NO$_x$ correlation equations are developed. The effect of inlet pressure and temperature are examined in the context of the correlation equations. Then, the LTO emissions for the V4 configuration are estimated and compared to the CAEP/6 standard. Finally, the NO$_x$ emissions from V4 are compared to those from V3.

CO emissions and combustion efficiency   At high power, the CO emissions were very low; the median value was 4 ppm and the maximum value was only 25 ppm. Therefore, CO emissions will be presented in summary form, using a comparison to the equilibrium CO as calculated by CEA. As Fig. 6 shows, the measured CO is close to the equilibrium value at all conditions[7]. The combustion efficiency is estimated to be greater than 99.95% at all points.

Effect of fuel staging   Figures 7 and 9d show the effect of fuel staging, i.e. of changing the local equivalence ratio of the pilot stage fuel-air mixers relative to the equivalence ratio of the main stage fuel-air mixers. In the figure legends, the staging is indicated by stating how lean or how rich the pilot is compared to all the overall equivalence ratio[8].

---

[7]The discrepancies are small and can be ignored, due to the uncertainty in both the measurements and the calculations: the measured CO was less than 0.3% of the 1,000 ppm minimum range of the analyzer, and Jet-A is a multicomponent fuel that is only approximated by the CEA Jet-A entry.

[8]For example, if the local equivalence ratio for the pilots was 0.42 but the overall equivalence ratio was 0.40, the legend would include "pilot 5% rich".

If all fuel-air mixers mixed the fuel and air equally well, NO$_x$ emissions would be lowest when all fuel-air mixers were fueled equally. Even if some fuel-air mixers had only slightly better fuel-air mixing, increasing the fuel flow to these "good" fuel-air mixers while decreasing the fuel flow to the "almost-as-good" fuel-air mixers might not decrease the overall NO$_x$ emissions: since NO$_x$ is an exponential function of adiabatic flame temperature, the increase in the local flame temperature at the "good" fuel-air mixers might actually increases NO$_x$ emissions.

For V4, NO$_x$ emissions were at or near a minimum when the local equivalence ratio was the same for all stages. The most extensive data set showing the effect of staging was done at the inlet temperature for 85% power, as shown in Figure 7. For both inlet pressures shown, the most even fuel staging had slightly lower NO$_x$ emissions than any of the other fuel stagings. Very limited fuel staging was also done at the inlet temperature for 100% power; the fuel staging points are circled in Fig. 9d. At all of these points, the pilot stage was richer than the overall equivalence ratio. Due to the small number of points where the fuel staging is varied, the only conclusion that can be drawn here is that the effect of fueling staging is small.

Development and evaluation of NO$_x$ correlation equations   Correlation equations were developed allow the NO$_x$ emissions to be estimated at conditions other than the conditions tested. In this paper, the correlation equations will be used to estimate the NO$_x$ emissions at the ICAO 85% and 100% power conditions. NO$_x$ correlation equations are also used to estimate emissions during flight and for other engine cycles. The form of the correlation equations used for estimating NO$_x$ is taken from the forms developed for first-generation SV-LDI-1, second-generation SV-LDI-2, and the V3 configuration [8, 12–14]. The form of the correlation equations is:

$$\mathrm{NO_x, EI} = p_3^a e^{(T_3/b)} \Delta p^c \left[d_p e^{(T_{\mathrm{ad,\,p}}/e_p)} + \right.$$
$$\left. 4 d_m e^{(T_{\mathrm{ad,\,m1}}/e_m)} + 6 d_m e^{(T_{\mathrm{ad,\,m2}}/e_m)} + 6 d_m e^{(T_{\mathrm{ad,\,m3}}/e_m)} \right], \quad (3)$$

where the combustor inlet temperature p_3 is in bars, the combustor inlet temperature T_3 is in Kelvin, the air pressure drop Δp is in percent of p_3, and the adiabatic flame temperature T_{ad} is in Kelvin. The subscripts p and m refer to the pilot and main stages, respectively. The local adiabatic flame temperature is calculated separately for each stage, with $T_{\mathrm{ad,\,p}}$ being the adiabatic flame temperature for the pilot stage and $T_{\mathrm{ad,\,m1}}$, $T_{\mathrm{ad,\,m2}}$, and $T_{\mathrm{ad,\,m3}}$ being the adiabatic flame temperatures for stages main 1, main 2, and main 3. The constants used to weight the main stages are the numbers of fuel-air mixers in each stage. The other values — a, b, c, d_p, d_m, e_p, and e_m — are the parameters of the correlation equations. These parameters are set based on a least-squares optimization or, in the case of a, b, and c, on previous experience.
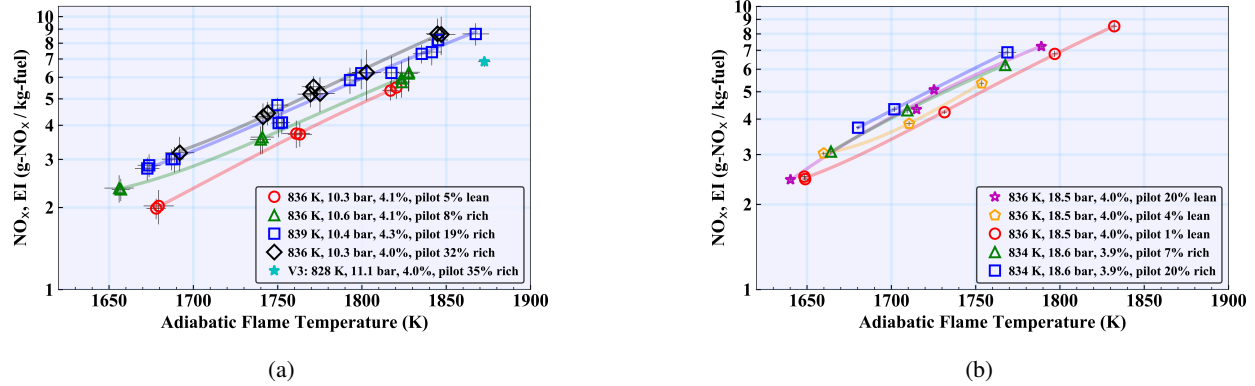
FIGURE 7: Effect of fuel staging on NO_x emissions at inlet pressures of (a) 10.5 bar and (b) 18.5 bar. The numbers in the legends are combustor inlet temperature, combustor inlet pressure, combustor pressure drop as a percentage of combustor inlet pressure, and the amount the pilot is lean or rich with respect to the overall equivalence ratio.

Three variations of the correlation equations were developed, labeled Fit 1, Fit 2, and Fit 3. For Fit 1, the parameters a, b, and c set to the values used for the SV-LDI-1 and SV-LDI-2 correlation equations [12, 13]. For Fit 2, parameters a, b, and c are set to the values used for V3 [14]. For both Fit 1 and Fit 2, an optimization was done on d_p, e_p, d_m, and e_m. For Fit 3, optimization was done on all 7 parameters[9]. The fit parameters are tabulated in Table 2 and the quality of the correlation equations is visualized in Fig. 8. Fit 2 is obviously lacking, with a R^2 of only 0.872[10]. Fits 1 and 3 have reasonable R^2 values, above 0.95 and are used to estimate the NO_x emissions at the 85% and 100% power ICAO points.

In the NO_x correlation equation, eq. 3, NO_x is approximated as a function of p_3^a, where a is 0.5 for Fit 1 and 0.52 for Fit 3. As stated in the Introduction, this simple dependence on p_3 does not make sense from a combustion science perspective. Nevertheless, approximations of the form $NO_x, EI = p^a h(\text{other variables}) + K$ are widely used. Here, p is either p_3 or the static or total ambient pressure at altitude, p_{amb}, and a and K are constants. Of the 15 NO_x approximation methods compiled by Chandrasekaran and Gupta [17], 13 are of this form. In particular, two important types of methods are of this form and have $K = 0$: (1) the P_3-T_3 method recommended by Chandrasekaran and Gupta as most accurate and (2) the fuel flow methods widely used by researchers studying the effect of air travel on the atmosphere and climate.

The accuracy of $NO_x \propto p_3^a$ can be evaluated by taking the ratio of NO_x emissions at two inlet pressures when all other parameters are matched. This is done in Fig. 9a-c; to help the reader, the pressure exponent a is calculated at several points.

The a values calculated this way vary substantially, from a=0.4 to nearly 1. In fact, the lowest value of a is even below 0.4. In Fig. 9a, the NO_x emissions at 14.0 bar are so close to those at 10.4 bar that $a \approx 0$ is the best estimate. The NO_x emissions do increase when the pressure is increased to 18.6 bar. This leads to very different estimates of a depending on whether the emissions at 18.6 bar are compared to those at 10.4 bar (a=0.4 to 0.6) or 14.0 bar (a=0.6 to 1). Although the inlet pressure seems to be the largest factor in determining a, fuel staging and adiabatic flame temperature also seem to have at effect, as can be seen by comparing the emissions at 10.5 bar to those at 18.6 bar. When the pilot is rich relative to the overall equivalence ratio and the flame temperature is below 1700 K, a is near 0.45; otherwise, a is near 0.7. Since the data show a varying between 0 and 1, the a values of 0.5 and 0.52 used in the correlation equations Fit 1 and Fit 3 seem reasonable; however, using $a \approx 0.5$ is unlikely to capture the difference between any two matched points. More generally, most correlation methods use an a between 0.4 and 0.6 [17]. Researchers using the NO_x correlation equations could consider also using $a = 0$ and $a = 1$ to put approximate error bounds on the NO_x emissions.

Figure 9d shows the effect of inlet temperature on NO_x emissions. The limited available data indicate NO_x emissions are a nearly constant function of inlet temperature.

LTO NO_x emissions The key programmatic goal of V4 testing was to see if this combustor configuration met the AATT project goal of 80% NO_x reduction with respect to the CAEP/6 standard. NO_x emissions are given in Table 3 for each of the four ICAO power conditions. For the 85% and 100% power conditions, NO_x emissions could not be measured directly because the combustor inlet pressure was above the maximum allowable pressure for the flametube. Therefore, NO_x emissions at these

---

[9]But note that the accuracy of parameter c is unlikely to be good because the pressure drop was kept near 4%.

[10]R^2, the coefficient of determination, is a measure of the goodness of fit that varies from 0 (poor fit) to 1 (good fit).

TABLE 2: Values of constants used in the NO$_x$ correlation equation, eq. 3, and the R^2 measure of the goodness of fit.

Configuration	Fit	a	b	c	d_p	e_p	d_m	e_m	R^2
SV-LDI-3-4	Fit 1	0.500	340	-0.600	1.12×10^{-5}	210	2.41×10^{-7}	162	0.962
SV-LDI-3-4	Fit 2	0.931	234	-0.829	2.00×10^{-6}	209	5.39×10^{-9}	139	0.872
SV-LDI-3-4	Fit 3	0.520	215	-0.111	4.48×10^{-7}	190	4.54×10^{-8}	169	0.971
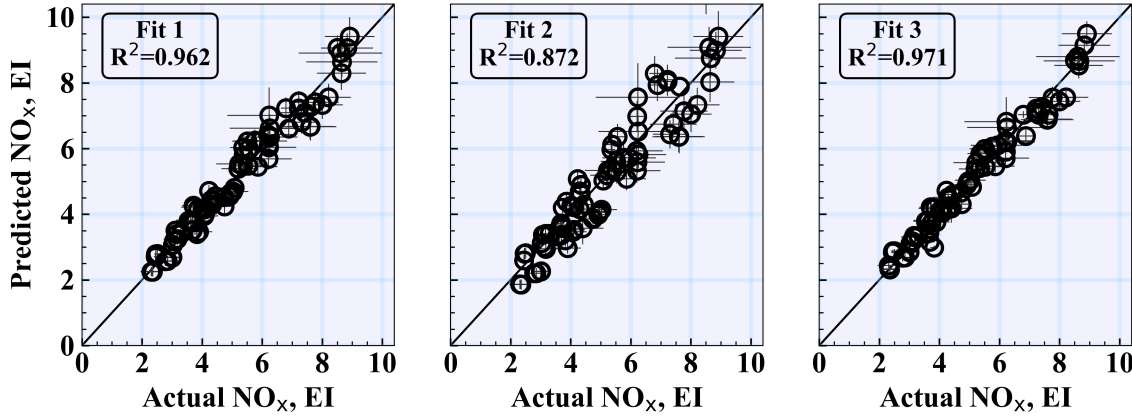
FIGURE 8: Evaluation of correlation equations: NO$_x$ "predicted" from correlation equations (form given in eq. 3 and constants in Table 2) vs measured values for Fit 1 (left), Fit 2 (center), and Fit 3 (right).

two power conditions were estimated four ways. The first two estimates used correlation equations (Fit 1 and Fit 3) developed to fit the high power emissions data. The other two estimates extrapolated NO$_x$ from the measured data using NO$_x \propto p_3^a$, with a=0.7 and a=1. The value a=0.7 was used because it was the typical value found when the adiabatic flame temperature was above 1700 K. The value a=1 was used because it was slightly higher than the highest a value found by examining the data; thus, it should serve as an upper bound for NO$_x$ emissions. LTO NO$_x$ emissions are estimated to be 85-90% below the CAEP/6 standard, exceeding the 80% NO$_x$ reduction goals set by AATT[11].

Comparison with V3 High power emissions for V3 are similar to those from V4. NO$_x$ emissions for V3 are compared with those in V4 in Fig. 9 parts c and d, showing V4 and V3 have similar high power NO$_x$ emissions. The high power combustion efficiency of V3 is also similar to that of V4, with both greater

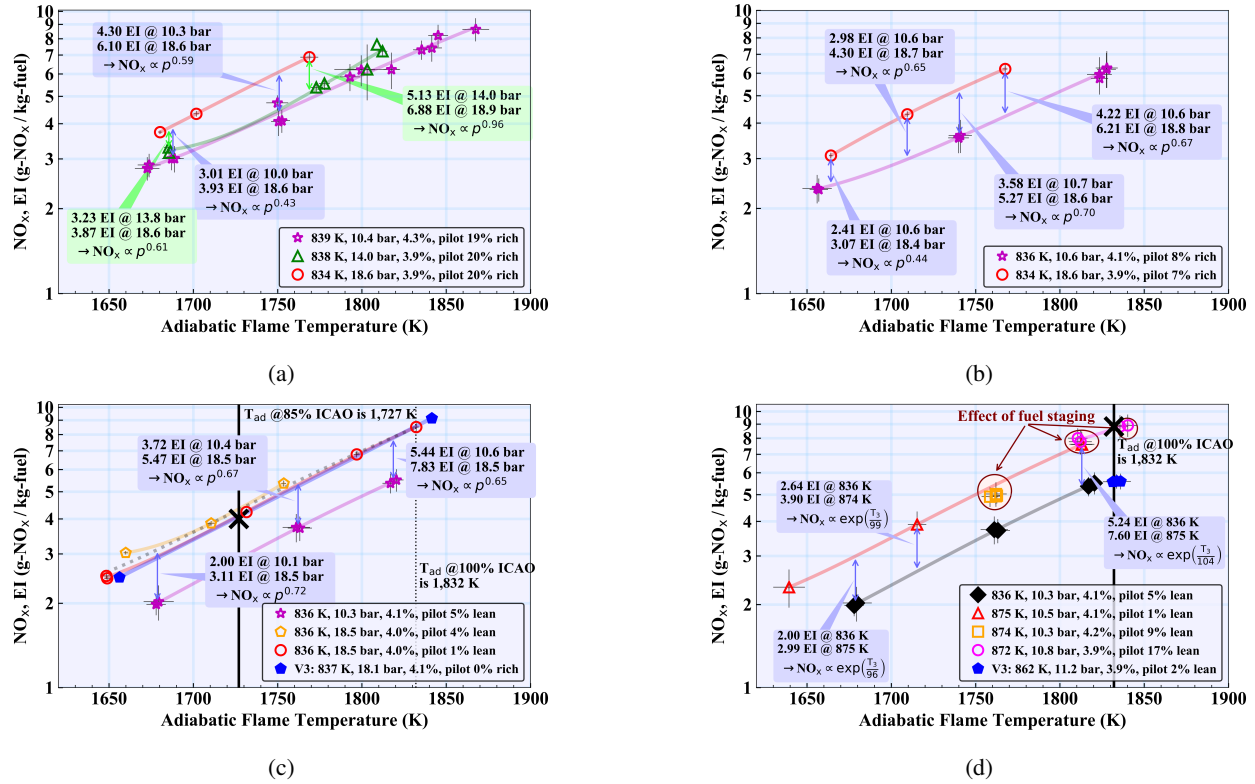than 99.95% [14]. The similar high power NO$_x$ emissions lead to an similar estimate of LTO NO$_x$ reduction. Both V3 and V4 have NO$_x$ reductions of 85-90% with respect to the CAEP/6 standard.

CONCLUSIONS

A third-generation swirl-venturi lean direct injector (SV-LDI-3) combustor concept was tested in the medium pressure flametube at the NASA Glenn Research Center. This concept is designated V4. It was compared with both the AATT NO$_x$ reduction goals and with a previous third-generation SV-LDI concept designated V3. Both V3 and V4 had similar landing-takeoff NO$_x$ levels: a reduction of 85-90% with respect to the CAEP/6 standard, exceeding the AATT goal of 80% NO$_x$ reduction. Both also had 99.95% combustion efficiency at high power. At the 7% ICAO low power condition, V4 had lower NO$_x$ emissions but unacceptably high CO and UHC emissions. Thus, overall, V4 did not perform better than V3.

Since correlation equations of the form NO$_x$ = $p^a h$(other variable) are widely used, the accuracy of NO$_x \propto p_3^a$ was evaluated by comparing NO$_x$ emissions at points matched in all variables except p$_3$ and computing a. It was found that a

---

[11]It is well known that this type of extrapolation is not highly accurate. The way the NO$_x$ reduction is stated "85-90% reduction" reflects this uncertainty. There are many other sources of uncertainty when going from a ceramic-lined flametube to a full engine, including the effects of going to a full-annular design and the effects of combustor liner cooling.

FIGURE 9: Effect of inlet pressure and temperature on NO_x emissions. Parts a-c show the effect of inlet pressure at the 85% power inlet temperature. Part d shows the effect of increasing the inlet temperature from the 85% power inlet temperature to the 100% power inlet temperature. To a very limited extent, it also shows the effect fuel staging. The black x on parts c and d mark the NO_x value used in the estimation of NO_x emissions at the 85% and 100% ICAO points, respectively.

TABLE 3: LTO NO_x emissions for V4.

ICAO point	Time (min)	Fuel flow (kg/min)	NO_x, EI (g/kg)				
			Meas	$NO_x \propto p_3^{0.7}$	$NO_x \propto p_3$	Fit1	Fit3
7%	26.0	3.68	3.45				
30%	4.00	11.3	3.0				
85%	2.20	38.1		5.97	7.09	6.12	6.18
100%	0.700	47.2		21.3	31.2	13.6	14.5
D_p/F_{00} (g/kN)				12.5	15.7	10.7	11.0
NO_x Reduction (%)				88.5	85.6	90.2	89.9

was not constant. Instead, a varied between 0 and 1. Typically, correlation equations used an a value near 0.5. By using a=0 and a=1 in addition, engine system analysts and researchers studying the effects of aircraft NO_x emmissions on the climate could provide error bounds.

REFERENCES

[1] Dahlmann, K., Grewe, V., Ponater, M., and Matthes, S., 2011. "Quantifying the contributions of individual NOx sources to the trend in ozone radiative forcing.". *Atmospheric Environment,* *45*, pp. 2860–2868.

[2] Lee, C.-M., Chang, C., Kramer, S., and Herbon, J. T., 2013. NASA project develops next-generaton low-emission combustor technologies. AIAA-2013-0540.

[3] He, Z. J., 2017. NOx emissions characteristics and correlation equations of two P&W axially staged sector combustors developed under NASA Environmentally Responsible Aviation ERA project. NASA/TM—2017-219381.

[4] Tacina, R. R., 1990. Low-NOx potential of gas turbine engines. AIAA-1990-0550.

[5] Tacina, R. R., 1990. Combustor technology for future aircraft. AIAA-1990-2440/NASA TM 103268.

[6] Tacina, R., Wey, C., Laing, P., and Mansour, A., 2005. A low-NOx lean-direct injection, multipoint integrated module combustor concept for advanced aircraft gas turbines. NASA/TM–2002-211347.

[7] Tacina, R., Mao, C.-P., and Wey, C., 2004. Experimental investigation of a multiplex fuel injector module with discrete jet swirlers for low emissions combustors. AIAA-2004-0135.

[8] Tacina, R., Lee, P., and Wey, C., 2005. A lean-direct-injection combustor using a 9 point swirl-venturi fuel injector. ISABE-2005-1106.

[9] Mansour, A., 2015. Development of advanced low emissions injectors and high-bandwidth fuel modulation flow valves. NASA/CR—2015-218899.

[10] Goeke, J., Pack, S., Zink, G., and Ryon, J., 2014. Multipoint combustion system final report. NASA/CR-2014-218112.

[11] Zink, G. A., Ryon, J. A., and Pack, S. D., 2014. Intermediate pressure combustion research of a multipoint low NOx combustion system. AIAA 2014-3629.

[12] Tacina, K. M., Lee, P., Mongia, H., Chang, C. T., He, Z., and Dam, B., 2014. A second generation swirl-venturi lean direct injection combustion concept. AIAA 2014-3434.

[13] Tacina, K. M., Lee, P., Mongia, H., He, Z., Podboy, D. P., and Dam, B., 2016. A comparison of three second-generation swirl-venturi lean direct injection combustor concepts. AIAA 2016-4891.

[14] Tacina, K., Podboy, D., Lee, F., and Dam, B., 2017.

[15] Tacina, K. M., 2012. Swirl-venturi lean direct injection combustion technology. Spring Technical Meeting of the Central States Section of the Combustion Institute.

[16] DuBois, D., and Paynter, G. C., 2006. ""Fuel Flow Method2" for Estimating Aircraft Emissions". *SAE Transactions: Journal of Aerospace,* *115*, pp. 1–14.

[17] Chandrasekaran, N., and Guha, A., 2012. "Study of prediction methods for NOx emissions from turbofan engines". *Journal of Propulsion and Power,* *28*, pp. 170–180.

[18] Lukachko, S., and Waitz, I., 2007. Effects of engine aging on aircraft NOx emissions. GT-386.

[19] Ajmani, K., Mongia, H., and Lee, P., 2017. CFD evaluation of a 3rd generation LDI combustor. AIAA 2017-5017.

[20] Ajmani, K., Mongia, H., Lee, P., and Tacina, K. CFD-led designs of pre-filming injectors for gas-turbine combustors. GT2018-75329.

[21] Ajmani, K., Lee, P., Mongia, H., and Tacina, K. CFD predictions of N+3 cycle emissions for a three-cup gas-turbine combustor. AIAA 2018-5429.

[22] SAE E-31 Technical Committee, 2011. Procedure for the continuous sampling and measurement of gaseous emissions from aircraft turbine engines. SAE ARP 1256D.

[23] SAE E-31 Technical Committee, 2013. Procedure for the analysis and evaluation of gaseous emissions from aircraft engines. SAE ARP 1533B.

[24] McBride, B., and Gordon, S., 1992. Computer program for calculating and fitting thermodynamic functions. NASA RP-1271.

[25] McBride, B., Zehe, M., and Gordon, S., 1993. NASA Glenn coefficients for calculating thermodynamic properties of individual species. NASA TP-3287.

[26] Walt, S. v. d., Colbert, S. C., and Varoquaux, G., 2011. "The numpy array: A structure for efficient numerical computation". *Computing in Science and Engineering,* *13*(2), pp. 22–30.

[27] Jones, E., Oliphant, T., Peterson, P., et al., 2001–. SciPy: Open source scientific tools for Python. [Online; accessed 26 October 2018].

[28] Hunter, J. D., 2007. "Matplotlib: A 2d graphics environment". *Computing In Science & Engineering,* *9*(3), pp. 90–95.

[29] McKinney, W., 2010. "Data structures for statistical computing in python". In Proceedings of the 9th Python in Science Conference, S. van der Walt and J. Millman, eds., pp. 51 – 56.

[30] Pérez, F., and Granger, B. E., 2007. "IPython: a system for interactive scientific computing". *Computing in Science and Engineering,* *9*(3), May, pp. 21–29.

Gaseous emissions results from a three-cup flametube test of a third-generation swirl-venturi lean direct injection combustion concept. ISABE-2017-22606.